Prediction of the Ω_{bbb} mass from lattice QCD

Stefan Meinel

Department of Physics, College of William & Mary, Williamsburg, Virginia 23187-8795, USA
(Received 28 October 2010; published 29 December 2010)

The mass of the triply-heavy baryon Ω_{bbb} is calculated in lattice QCD with $2+1$ flavors of light sea quarks. The b quark is implemented with improved lattice nonrelativistic QCD. Gauge field ensembles from both the RBC/UKQCD and MILC collaborations with lattice spacings in the range from 0.08 fm to 0.12 fm are used. The final result for the Ω_{bbb} mass, which includes an electrostatic correction, is $14.371 \pm 0.004_{\text{stat}} \pm 0.011_{\text{syst}} \pm 0.001_{\text{exp}}$ GeV. The hyperfine splitting between the physical $J = 3/2$ state and a fictitious $J = 1/2$ state is also calculated.

I. INTRODUCTION

Hadrons containing only heavy valence quarks play a key role in the study of QCD due to their approximately nonrelativistic nature and their clean spectrum of narrow states. Many precise experimental results are available for heavy quarkonium mesons, and their analysis has contributed significantly to the understanding of the quark-antiquark forces [1,2]. However, the nature of the QCD gauge symmetry is exhibited in the most direct way in the *baryons*, where the number of valence quarks is equal to the number of colors. It is therefore of great interest to explore triply-heavy baryons like the Ω_{bbb}. Masses and other properties of triply-heavy baryons have been calculated using various quark models [3–18] and sum rules [19]. Most potential-model calculations include only two-body forces, but QCD also leads to genuine three-body forces. A three-body linear confinement term was found in the static three-quark potential calculated nonperturbatively from lattice QCD [20]. In perturbative QCD, three-body forces first arise at next-to-next-to-leading order [21].

Triply-heavy baryons have not yet been observed experimentally (see [5,22–25] for experimental aspects and calculations of production rates in colliders), and the predictions of their properties cannot yet be compared to the real world. The model-dependent calculations can however be tested by comparing them to nonperturbative first-principles calculations in lattice QCD.

While there are several recent lattice QCD calculations of singly- and doubly-heavy baryon masses [26–31], there appears to be only one lattice result for a triply-heavy baryon mass in the literature so far: the Ω_{ccc} in Ref. [32]. The calculation in [32] was performed in the quenched approximation, i.e. neglecting the effects of dynamical light quarks, and the result for $M_{\Omega_{ccc}}$ obtained there may also have significant discretization errors [33] due to the use of a relativistic action for the charm quark at the rather large value of $am_c = 0.8$ (where m_c is the bare charm quark mass and a is the lattice spacing).

In the following, a precise calculation of the mass of the triply-bottom baryon Ω_{bbb} in lattice QCD with $2+1$ flavors of dynamical light quarks is reported (a preliminary result was given in [34]). The hyperfine splitting between the Ω_{bbb} baryon with $J = 3/2$ and a fictitious $J = 1/2$ state composed of three heavy quarks with the same mass as the b quark is also calculated. The computations are performed at lattice spacings in the range from approximately 0.08 fm to 0.12 fm. At these values of the lattice spacing, the b quark can be implemented very accurately with lattice nonrelativistic QCD (NRQCD) [35–37]. Most of the calculations in this work are done on gauge field ensembles that were generated by the RBC and UKQCD collaborations using the Iwasaki action for the gluons and a domain-wall action for the sea quarks [38,39]. As a test of universality, calculations are also performed on gauge field ensembles generated by the MILC Collaboration using the Lüscher-Weisz action for the gluons and a rooted staggered action for the sea quarks [40]. The details of the gauge field ensembles are given in Sec. II. The mass of the Ω_{bbb} is obtained by calculating the difference $E_{\Omega_{bbb}} - \frac{3}{8}(E_{\eta_b} + 3E_{\Upsilon})$, as described in Sec. III. This quantity has only a weak dependence on the b quark mass and on the light quark masses, as demonstrated by the lattice results in Sec. IV. In the final result for $M_{\Omega_{bbb}}$, a correction due to the electrostatic Coulomb interaction of the b quarks is included (Sec. V).

II. LATTICE ACTIONS AND PARAMETERS

The problem with heavy quarks on the lattice is that relativistic actions develop large discretization errors when the heavy-quark mass becomes comparable to the inverse lattice spacing. In this work, the b quarks are therefore implemented with lattice NRQCD [35,36], a nonrelativistic effective field theory for heavy quarks. Unlike the heavy quark effective theory developed in [41], which is limited to heavy-light hadrons, NRQCD can be applied to hadrons containing any number of heavy quarks. The use of NRQCD to study triply-heavy baryons has already been suggested in [35]. The power counting in this case should be very similar to that for heavy quarkonia, and is given in terms of the typical heavy-quark velocity inside the hadron. For bottomonium, one has $v^2 \approx 0.1$ (in units with $c = 1$), and the value is expected to be comparable

for the Ω_{bbb} [the length scales are similar; see Eqs. (17) and (18) in Sec. V].

The NRQCD action employed here includes all terms up to order v^4, as well as Symanzik-improvement corrections (which reduce discretization errors). The matching to QCD is performed at tree level, and the action is tadpole-improved using the mean link u_{0L} in Landau gauge [42,43]. The action is equal to the one used in [37], with $c_1 = c_2 = c_3 = c_4 = c_5 = c_6 = 1$ and $c_7 = c_8 = c_9 = 0$ (in the notation used there.) For comparison, some results obtained with the order-v^2 action, which has $c_5 = c_6 = 1$ and $c_1 = c_2 = c_3 = c_4 = c_7 = c_8 = c_9 = 0$, will also be given.

The details of the gauge field ensembles used in this work are shown in Table I. All ensembles include the effects of dynamical up-, down-, and strange sea quarks (with $m_u = m_d$, in the following denoted as m_l). The ensembles generated by the RBC and UKQCD collaborations [38,39] make use of a domain-wall action [47–49] for the sea quarks, and the Iwasaki action [50,51] for the gluons. The domain-wall action yields an exact chiral symmetry when the extent L_5 of the auxiliary fifth dimension is taken to infinity. The Iwasaki action suppresses the residual chiral symmetry breaking at finite L_5 [52] (here, $L_5 = 16$).

Calculations are also performed on two ensembles generated by the MILC Collaboration [40], using the AsqTad action [53–55] in combination with the rooting procedure [40] for the sea quarks, and the tadpole-improved Lüscher-Weisz action [56–58] for the gluons. By comparing the results from the RBC/UKQCD and from the MILC ensembles, sea-quark and gluon discretization effects can be disentangled from NRQCD discretization effects [37].

Table I also shows the lattice spacings of the ensembles, determined from the $\Upsilon(2S) - \Upsilon(1S)$ splitting [37], and the values of the bare b-quark mass in lattice units, am_b. The b-quark mass is set such that the kinetic mass of the $\eta_b(1S)$

meson agrees with experiment within the statistical errors. The main calculations in this work are performed directly at the physical values of am_b as determined in [37]; additional results for other values of am_b will also be given to illustrate the dependence on am_b. On the coarse MILC ensemble, the value of am_b used here is 0.9% below the physical value obtained in [37].

III. CONSTRUCTION OF TWO-POINT FUNCTIONS AND ANALYSIS

The ground-state energies of the η_b, the Υ, and the Ω_{bbb} are extracted from fits to the Euclidean time-dependence of suitable two-point functions at zero momentum. On a given lattice gauge field configuration, the two-point functions for the η_b, the Υ, and the Ω_{bbb} are defined as

$$C^{(\eta)}(t, t', \boldsymbol{x}') = \sum_{\boldsymbol{x}} G^{\dagger ab}_{\alpha\beta}(t, \boldsymbol{x}, t', \boldsymbol{x}') G^{ba}_{\beta\alpha}(t, \boldsymbol{x}, t', \boldsymbol{x}'), \quad (1)$$

$$C^{(\Upsilon)}(t, t', \boldsymbol{x}') = \sum_{\boldsymbol{x}} (\gamma_j \gamma_5)_{\alpha\beta} G^{\dagger ab}_{\beta\gamma}(t, \boldsymbol{x}, t', \boldsymbol{x}')$$
$$\times (\gamma_5 \gamma_j)_{\gamma\delta} G^{ba}_{\delta\alpha}(t, \boldsymbol{x}, t', \boldsymbol{x}'), \quad (2)$$

$$C^{(\Omega)}_{jk\alpha\delta}(t, t', \boldsymbol{x}') = \sum_{\boldsymbol{x}} \epsilon_{abc} \epsilon_{fgh} (C\gamma_j)_{\beta\gamma} (\overline{C\gamma_k})_{\rho\sigma} G^{af}_{\beta\sigma}(t, \boldsymbol{x}, t', \boldsymbol{x}')$$
$$\times G^{bg}_{\gamma\rho}(t, \boldsymbol{x}, t', \boldsymbol{x}') G^{ch}_{\alpha\delta}(t, \boldsymbol{x}, t', \boldsymbol{x}'). \quad (3)$$

Here, $a, b, c, \ldots$ are color indices (running from 1 to 3), $\alpha, \beta, \gamma, \ldots$ are spinor indices (running from 1 to 4), $C = \gamma_0 \gamma_2$ is the (Euclidean) charge conjugation matrix, and the overline denotes the Dirac conjugate. The indices j, k are in the range from 1 to 3. In the nonrelativistic gamma-matrix basis used here, the NRQCD heavy-quark propagator G has vanishing lower spinor components (for $t > t'$),

TABLE I. Summary of lattice parameters. The bare gauge couplings are given as $\beta = 6/g^2$ (for the RBC/UKQCD ensembles) and $\beta = 10/g^2$ (for the MILC ensembles). For the RBC/UKQCD ensembles, the pion masses in lattice units were taken from [38,39,44] and converted to physical units using the lattice spacings given here. For the MILC ensembles, there are taste splittings between the different pions [40], and the root-mean-square masses taken from [45,46] are given.

Collaboration	$L^3 \times T$	β	am_l	am_s	am_b	u_{0L}	n_{conf}	a^{-1} (GeV)	m_π (GeV)
RBC/UKQCD	$16^3 \times 32$	2.13	0.01	0.04	2.469	0.8439	352	1.766(52)	0.436(14)
	$16^3 \times 32$	2.13	0.02	0.04	2.604	0.8433	355	1.687(46)	0.548(16)
	$16^3 \times 32$	2.13	0.03	0.04	2.689	0.8428	711	1.651(33)	0.639(14)
RBC/UKQCD	$24^3 \times 64$	2.13	0.005	0.04	2.487	0.8439	311	1.763(27)	0.3377(54)
	$24^3 \times 64$	2.13	0.01	0.04	2.522	0.8439	266	1.732(28)	0.4194(70)
	$24^3 \times 64$	2.13	0.02	0.04	2.622	0.8433	73	1.676(42)	0.541(14)
	$24^3 \times 64$	2.13	0.03	0.04	2.691	0.8428	72	1.650(39)	0.641(15)
RBC/UKQCD	$32^3 \times 64$	2.25	0.004	0.03	1.831	0.8609	314	2.325(32)	0.2950(40)
	$32^3 \times 64$	2.25	0.006	0.03	1.829	0.8608	296	2.328(45)	0.3529(69)
	$32^3 \times 64$	2.25	0.008	0.03	1.864	0.8608	270	2.285(32)	0.3950(55)
MILC	$24^3 \times 64$	6.76	0.005	0.05	2.64	0.8362	525	1.647(14)	0.460
MILC	$28^3 \times 96$	7.09	0.0062	0.031	1.86	0.8541	478	2.291(22)	0.416

$$G(t, \boldsymbol{x}, t', \boldsymbol{x}') = \begin{pmatrix} G_\psi(t, \boldsymbol{x}, t', \boldsymbol{x}') & 0 \\ 0 & 0 \end{pmatrix}, \qquad (4)$$

where G_ψ is the NRQCD propagator with two spinor components. The propagator G_ψ may include at the source and/or sink a Gaussian smearing operator

$$\left(1 + \frac{r_S}{n_S}\Delta^{(2)}\right)^{n_S}, \qquad (5)$$

where $\Delta^{(2)}$ is a covariant lattice Laplacian. The smearing is intended to improve the overlap with the ground state and reduce the contamination from excited states. For the meson two-point functions, smearing is only performed on G_ψ, not $G_\psi^\dagger$, while for the baryon two-point functions all three G_ψ's are treated equally.

When defined through Eq. (3), the two-point function $C_{jk\alpha\delta}^{(\Omega)}(t, t', \boldsymbol{x}')$ couples to both the physical spin-3/2 state Ω_{bbb}, and an unphysical spin-1/2 state (when all three quark flavors are equal, this state violates the Pauli exclusion principle). At large Euclidean time separation $t - t'$, the two-point function (after averaging over gauge configurations) approaches the form

$$C_{jk}^{(\Omega)} \to Z_{3/2}^2 e^{-E_{3/2}(t-t')} \frac{1}{2}(1 + \gamma_0)\left(\delta_{jk} - \frac{1}{3}\gamma_j\gamma_k\right)$$
$$+ Z_{1/2}^2 e^{-E_{1/2}(t-t')} \frac{1}{2}(1 + \gamma_0)\frac{1}{3}\gamma_j\gamma_k, \qquad (6)$$

where $E_{3/2} = E_{\Omega_{bbb}}$ and $E_{1/2}$ are the ground-state energies of the $J = \frac{3}{2}$ and $J = \frac{1}{2}$ states, respectively (see for example [59]). The $J = \frac{3}{2}$ and $J = \frac{1}{2}$ contributions can be disentangled by multiplying with the projectors

$$P_{ij}^{(3/2)} = \left(\delta_{ij} - \frac{1}{3}\gamma_i\gamma_j\right), \qquad (7)$$

$$P_{ij}^{(1/2)} = \frac{1}{3}\gamma_i\gamma_j, \qquad (8)$$

which gives

$$P_{ij}^{(J)}C_{jk}^{(\Omega)} \to Z_J^2 e^{-E_J(t-t')} \frac{1}{2}(1 + \gamma_0)P_{ik}^{(J)}. \qquad (9)$$

Before the fitting, an average over all nonvanishing spinor and Lorentz components is calculated, which is defined as

$$\langle P^{(J)}C^{(\Omega)}\rangle = \sum_{\substack{i, k, \alpha, \delta, \\ [(1 + \gamma_0)P_{ik}^{(J)}]_{\alpha\delta} \neq 0}} \frac{[P_{ij}^{(J)}C_{jk}^{(\Omega)}]_{\alpha\delta}}{[(1 + \gamma_0)P_{ik}^{(J)}]_{\alpha\delta}}. \qquad (10)$$

In order to increase statistics, the two-point functions are calculated for 32 different source locations $(t', \boldsymbol{x}')$ spread evenly across the lattice on each gauge field configuration. The source locations are shifted randomly from configuration to configuration. No significant autocorrelations were seen either between source locations or in molecular dynamics time. An example of a matrix of Ω_{bbb} two-point functions is shown in Fig. 1. The four different functions correspond to smeared or local sources and/or sinks. The data are fitted by a sum of exponentials using the Bayesian technique from [60]. The fit functions and priors are chosen as discussed in [61].

Because of the use of NRQCD, the energies extracted from fits of two-point functions contain a shift that is proportional to the number of heavy quarks in the hadron. This shift cancels in the energy differences

$$aE_{\Omega_{bbb}} - \frac{3}{8}(aE_{\eta_b} + 3aE_\Upsilon) \qquad (11)$$

and

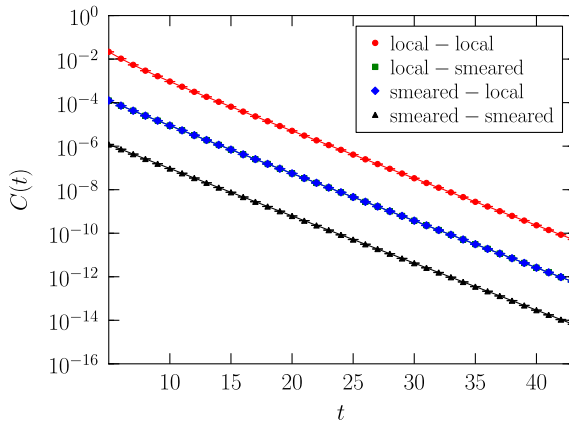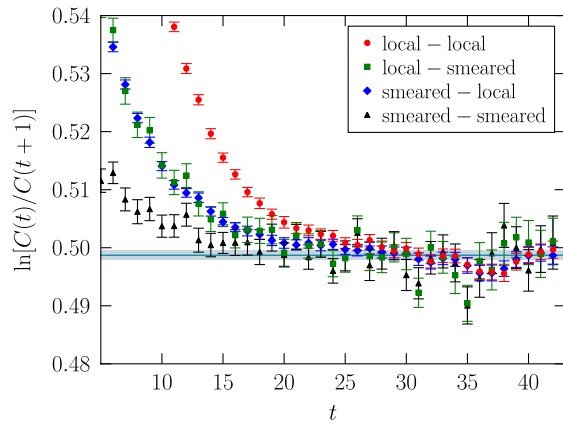$$aE_{\Omega_{bbb}} - \frac{3}{2}aE_\Upsilon. \qquad (12)$$

FIG. 1 (color online). Left panel: matrix of Ω_{bbb} two-point functions $C(t) = \langle P^{(3/2)}C^{(\Omega)}\rangle$ with local and smeared interpolating fields (the local-smeared and smeared-local data coincide); the lines are from a fit with 7 exponentials and $t_{\min} = 5$. Right panel: corresponding effective-energy plot and ground-state energy. The data are from the RBC/UKQCD ensemble with $L = 32$, $am_l = 0.004$. Lattice units are used.

As will be shown in Sec. IV, the quantity (11), which contains the spin average of the $1S$ bottomonium states, has a weaker dependence on the b-quark mass than (12) and is therefore preferred for the determination of $M_{\Omega_{bbb}}$. The energy differences (11) and (12) are computed using statistical bootstrap in order to take into account correlations.

After conversion to physical units using the lattice spacings from the $\Upsilon(2S) - \Upsilon(1S)$ splittings, the data from the RBC/UKQCD ensembles are extrapolated linearly in m_π^2 to the physical pion mass. As in [37], the data from the $L = 24$ and $L = 32$ ensembles, which have the same physical box size, are extrapolated simultaneously, allowing for an arbitrary dependence on the lattice spacing a. Higher-order terms depending on both a and m_π are neglected.

IV. LATTICE RESULTS

The lattice results for the energy differences (11) and (12), and the unphysical spin splitting $aE_{\Omega_{bbb}} - aE_{1/2}$ are given in Table II. On the RBC/UKQCD ensembles with $L = 24$, $am_l = 0.005$ and $L = 32$, $am_l = 0.004$, results for multiple values of am_b are listed. The quark-mass-dependence of (11) and (12) is visualized in Fig. 2. As can be seen there, the dependence on am_b is smaller for (11). The quark-mass-dependence of the hyperfine splitting $aE_{\Omega_{bbb}} - aE_{1/2}$ is visualized in Fig. 3. As can be seen in the plot, the dependence is slightly weaker than $1/(am_b)$, similarly to the $1S$ hyperfine splitting in bottomonium [37]. The data are described well by fits with the function $A/(am_b) + B$.

On the $L = 24$, $am_l = 0.005$ and $L = 32$, $am_l = 0.004$ ensembles, results calculated with the leading-order (order-v^2) NRQCD action are also given in Table II. This action does not contain spin-dependent terms, so that $aE_{\Omega_{bbb}} - aE_{1/2} = 0$ and $aE_\Upsilon - aE_{\eta_b} = 0$, and consequently the quantities (11) and (12) become equal. Remarkably, for the splitting $aE_{\Omega_{bbb}} - \frac{3}{8}(aE_{\eta_b} + 3aE_\Upsilon)$ the results obtained at the same value of am_b with the order-v^4 and with the order-v^2 actions differ by less than 1%. It appears that there is a large cancellation of the order-v^4 corrections in $aE_{\Omega_{bbb}}$ and $\frac{3}{8}(aE_{\eta_b} + 3aE_\Upsilon)$, which is another reason to use (11) for the determination of $M_{\Omega_{bbb}}$. On the other hand, for the splitting $aE_{\Omega_{bbb}} - \frac{3}{2}aE_\Upsilon$, the values obtained with the order-v^4 and with the order-v^2 actions differ by about 10%, as might be expected for $v^2 \approx 0.1$.

The results for $aE_{\Omega_{bbb}} - \frac{3}{8}(aE_{\eta_b} + 3aE_\Upsilon)$ and $aE_{\Omega_{bbb}} - aE_{1/2}$ from the order-v^4 action at the physical values of am_b were then converted to physical units using the inverse lattice spacing values from Table I. The chiral extrapolations of the data from the RBC/UKQCD ensembles are visualized in Figs. 4 and 5. As can be seen there, the dependence of the results on the pion mass is weak. This also indicates that the higher-order terms depending on both a and m_π are small. The data from the $L = 16$ ensembles, which provide a test of finite-volume effects, were extrapolated independently. No significant finite-volume effects are seen, as expected for the small size of the Ω_{bbb} and bottomonium ground states [Eqs. (17) and (18)].

TABLE II. Results in lattice units. The errors are statistical/fitting only.

| Collaboration	$L^3 \times T$	am_l	am_b	Action	$aE_{\Omega_{bbb}} - \frac{3}{8}(aE_{\eta_b} + 3aE_\Upsilon)$	$aE_{\Omega_{bbb}} - \frac{3}{2}aE_\Upsilon$	$aE_{\Omega_{bbb}} - aE_{1/2}$
RBC/UKQCD	$16^3 \times 32$	0.01	2.469	v^4	0.11690(65)	0.10527(64)	0.01364(30)
	$16^3 \times 32$	0.02	2.604	v^4	0.12063(65)	0.10934(64)	0.01399(31)
	$16^3 \times 32$	0.03	2.689	v^4	0.11972(57)	0.10856(56)	0.01357(28)
RBC/UKQCD	$24^3 \times 64$	0.005	2.3	v^4	0.11483(95)	0.10269(96)	0.01417(47)
	$24^3 \times 64$	0.005	2.487	v^4	0.11551(97)	0.10407(98)	0.01340(42)
	$24^3 \times 64$	0.005	2.487	v^2	0.11445(78)	0.11445(78)	0
	$24^3 \times 64$	0.005	2.536	v^4	0.11568(99)	0.10442(98)	0.01322(43)
	$24^3 \times 64$	0.005	2.7	v^4	0.11631(95)	0.10566(93)	0.01268(40)
	$24^3 \times 64$	0.01	2.522	v^4	0.11731(78)	0.10586(81)	0.01365(42)
	$24^3 \times 64$	0.02	2.622	v^4	0.1183(17)	0.1072(17)	0.01343(94)
	$24^3 \times 64$	0.03	2.691	v^4	0.1217(14)	0.1106(14)	0.01377(66)
RBC/UKQCD	$32^3 \times 64$	0.004	1.75	v^4	0.08427(74)	0.07463(75)	0.01045(47)
	$32^3 \times 64$	0.004	1.831	v^4	0.08453(76)	0.07521(77)	0.01012(49)
	$32^3 \times 64$	0.004	1.831	v^2	0.08473(48)	0.08473(48)	0
	$32^3 \times 64$	0.004	1.87	v^4	0.08466(72)	0.07549(74)	0.00995(45)
	$32^3 \times 64$	0.004	2.05	v^4	0.08540(70)	0.07685(70)	0.00935(40)
	$32^3 \times 64$	0.006	1.829	v^4	0.08581(68)	0.07647(68)	0.01061(44)
	$32^3 \times 64$	0.008	1.864	v^4	0.08584(98)	0.07516(98)	0.01007(50)
MILC	$24^3 \times 64$	0.005	2.64	v^4	0.12447(64)	0.11216(64)	0.01438(30)
MILC	$28^3 \times 96$	0.0062	1.86	v^4	0.08757(49)	0.07786(50)	0.01022(24)
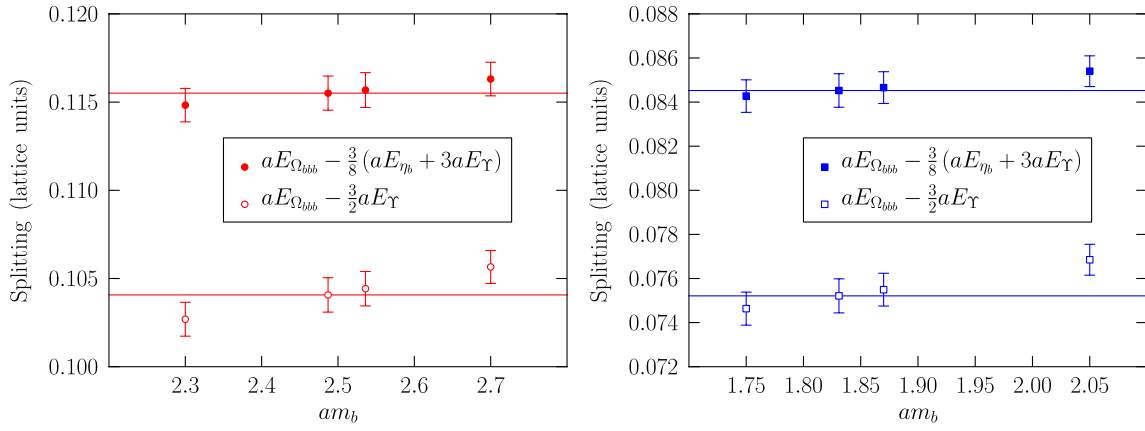
FIG. 2 (color online). Dependence of the quantities $aE_{\Omega_{bbb}} - \frac{3}{8}(aE_{\eta_b} + 3aE_\Upsilon)$ and $aE_{\Omega_{bbb}} - \frac{3}{2}aE_\Upsilon$ on the bare heavy-quark mass. Left panel: RBC/UKQCD $L = 24$, $am_l = 0.005$; right panel: RBC/UKQCD $L = 32$, $am_l = 0.004$. The lines indicate the values at the physical b-quark mass.
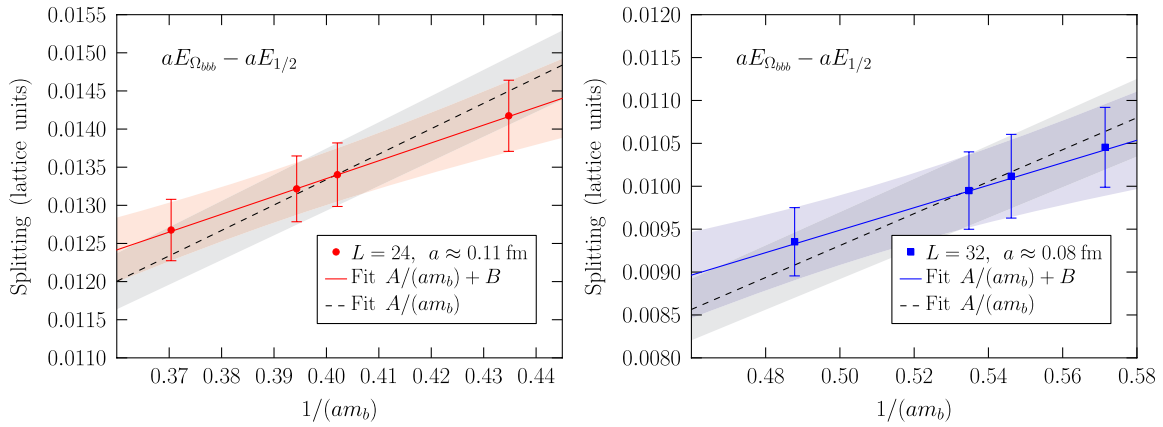

FIG. 3 (color online). Dependence of the (unphysical) spin splitting $aE_{\Omega_{bbb}} - aE_{1/2}$ on the bare heavy-quark mass. Left panel: RBC/UKQCD $L = 24$, $am_l = 0.005$; right panel: RBC/UKQCD $L = 32$, $am_l = 0.004$. Also shown are fits using the functions $A/(am_b)$ and $A/(am_b) + B$.
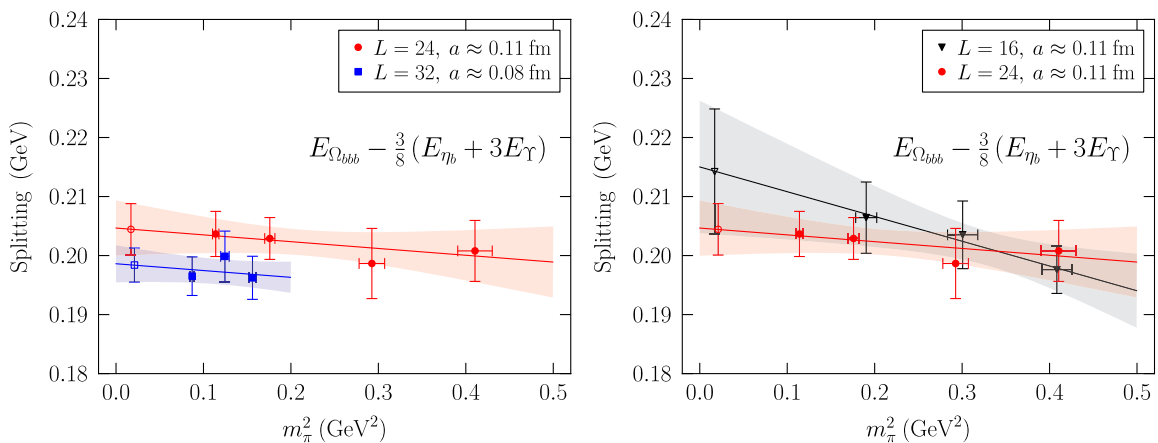

FIG. 4 (color online). Chiral extrapolation of the quantity $E_{\Omega_{bbb}} - \frac{3}{8}(E_{\eta_b} + 3E_\Upsilon)$ from the RBC/UKQCD gauge field ensembles. The extrapolated points are offset horizontally for legibility.
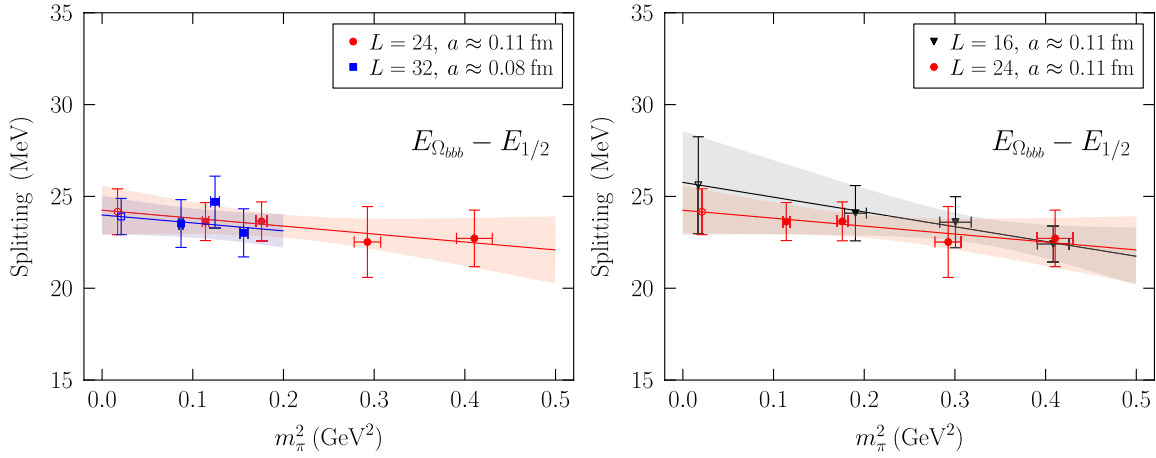
FIG. 5 (color online). Chiral extrapolation of the (unphysical) spin splitting $E_{\Omega_{bbb}} - E_{1/2}$ from the RBC/UKQCD gauge field ensembles. Extrapolated points are offset horizontally for legibility.

The results of the chiral extrapolations of $E_{\Omega_{bbb}} - \frac{3}{8}(E_{\eta_b} + 3E_\Upsilon)$ and $E_{\Omega_{bbb}} - E_{1/2}$ to $m_\pi = 138$ MeV are given in Table III. Also shown in the table are the results from the MILC ensembles, and the results from the $L = 24$ and $L = 32$ RBC/UKQCD ensembles after interpolation/extrapolation to $m_\pi = 460$ MeV and $m_\pi = 416$ MeV, respectively, so as to match the root-mean-square pion masses of the MILC ensembles. As mentioned above, on the coarse MILC ensemble the value of am_b used here is 0.9% below the physical value obtained in [37]. However, this affects the hyperfine splitting in physical units by only 0.2 standard deviations, which is negligible.

For the hyperfine splitting, no significant dependence on the lattice spacing is seen, and the results from the RBC/UKQCD and MILC ensembles at the matching pion masses are in agreement, indicating that gluon discretization errors for this quantity are small. However, for this splitting systematic errors of order $\alpha_s \approx 20$–30% and $v^2 \approx 10\%$ due to missing radiative and relativistic corrections in the NRQCD action are expected. The final result for the (fictitious) hyperfine splitting is then

$$E_{\Omega_{bbb}} - E_{1/2} = 24 \pm 1_{\text{stat}} \pm 6_{\text{syst}} \text{ MeV}. \tag{13}$$

The quantity $E_{\Omega_{bbb}} - \frac{3}{8}(E_{\eta_b} + 3E_\Upsilon)$ is seen to change by about 6 MeV (1.1σ) when going from the coarse to the fine lattice spacing on the RBC/UKQCD ensembles. At the coarse lattice spacing and at the matching pion masses, the results from the RBC/UKQCD and MILC ensembles differ by about 3 MeV (1.0σ); at the fine lattice spacing this difference is 4 MeV (1.2σ). Given that the ratio of a^2 between the fine and coarse lattices is about 2, it seems reasonable to assume a maximum total discretization error of 10 MeV (5%) for the result from the fine ($L = 32$) RBC/UKQCD ensemble. The systematic errors from the missing radiative and relativistic corrections in the NRQCD action can be estimated to be of order $\alpha_s v^2 \approx 2$–3% and $v^4 \approx 1\%$ respectively. Thus, the final result for $E_{\Omega_{bbb}} - \frac{3}{8}(E_{\eta_b} + 3E_\Upsilon)$ (without the electrostatic correction to be discussed in Sec. V) is

$$E_{\Omega_{bbb}} - \frac{3}{8}(E_{\eta_b} + 3E_\Upsilon) = 0.198 \pm 0.003_{\text{stat}} \pm 0.011_{\text{syst}} \text{ GeV}. \tag{14}$$

TABLE III. Values of $E_{\Omega_{bbb}} - \frac{3}{8}(E_{\eta_b} + 3E_\Upsilon)$ and $E_{\Omega_{bbb}} - E_{1/2}$ in physical units. The errors are statistical/fitting only. The first three rows of the table give the results from the RBC/UKQCD ensembles, extrapolated to the physical pion mass. In the remaining rows, the results from the MILC ensembles are compared to the results from the RBC/UKQCD ensembles; there, the RBC/UKQCD data were interpolated/extrapolated to match the root-mean-square pion masses of the MILC ensembles.

Collaboration	$L^3 \times T$	m_π (GeV)	$E_{\Omega_{bbb}} - \frac{3}{8}(E_{\eta_b} + 3E_\Upsilon)$ (GeV)	$E_{\Omega_{bbb}} - E_{1/2}$ (MeV)
RBC/UKQCD	$16^3 \times 32$	0.138	0.214(11)	25.6(2.6)
RBC/UKQCD	$24^3 \times 64$	0.138	0.2044(44)	24.2(1.2)
RBC/UKQCD	$32^3 \times 64$	0.138	0.1984(29)	23.91(99)
MILC	$24^3 \times 64$	0.460	0.2052(22)	23.69(65)
RBC/UKQCD	$24^3 \times 64$	0.460	0.2022(22)	23.33(63)
MILC	$28^3 \times 96$	0.416	0.2008(24)	23.41(72)
RBC/UKQCD	$32^3 \times 64$	0.416	0.1966(24)	23.24(84)

V. THE MASS OF THE Ω_{bbb}

The result (14) is the pure QCD value and needs to be corrected to include the effects of electromagnetism. Since the quarks in both the Ω_{bbb} and bottomonium are heavy and are moving slowly, the dominant electromagnetic correction is due to the electrostatic Coulomb interaction. The Coulomb interaction is repulsive in the Ω_{bbb} and it therefore increases $E_{\Omega_{bbb}}$. On the other hand, the Coulomb interaction is attractive in bottomonium and it therefore decreases E_{η_b} and E_Υ. Using $\langle \Upsilon | r^{-1} | \Upsilon \rangle = \langle \eta_b | r^{-1} | \eta_b \rangle$, the electrostatic correction to (14) becomes

$$E_{\text{Coulomb}} = 3 \frac{(e/3)^2}{4\pi\epsilon_0} \left\langle \Omega_{bbb} \left| \frac{1}{r} \right| \Omega_{bbb} \right\rangle$$
$$+ \frac{3}{2} \frac{(e/3)^2}{4\pi\epsilon_0} \left\langle \Upsilon \left| \frac{1}{r} \right| \Upsilon \right\rangle. \qquad (15)$$

Here, r is defined as the distance between two b quarks (for the Ω_{bbb}) or the distance between the b and $\bar{b}$ (for the Υ). The expectation value $\langle \Upsilon | r^{-1} | \Upsilon \rangle$ is calculated numerically using the $1S$ wave function obtained with the QQ-onia package [62] for the Cornell potential with parameters as in [62]. This gives

$$\left\langle \Upsilon \left| \frac{1}{r} \right| \Upsilon \right\rangle = 8.1 \text{ fm}^{-1}. \qquad (16)$$

In Ref. [9], the mean-square distance of a heavy quark from the center of mass in the Ω_{bbb} has been calculated using a potential model, with the result $\langle \Omega_{bbb} | r^2_{\text{CM}} | \Omega_{bbb} \rangle = 0.021 \text{ fm}^2$. The geometry of the system implies $r = \sqrt{3} r_{\text{CM}}$, and therefore

$$\sqrt{\langle \Omega_{bbb} | r^2 | \Omega_{bbb} \rangle} = 0.25 \text{ fm}. \qquad (17)$$

For comparison, in the Υ the wave function from QQ-onia gives

$$\sqrt{\langle \Upsilon | r^2 | \Upsilon \rangle} = 0.20 \text{ fm}. \qquad (18)$$

Therefore, in the following the estimate $\langle \Omega_{bbb} | r^{-1} | \Omega_{bbb} \rangle = (0.8 \pm 0.4) \langle \Upsilon | r^{-1} | \Upsilon \rangle = 6.5 \pm 3.2 \text{ fm}^{-1}$ is used. This gives

$$E_{\text{Coulomb}} = 5.1 \pm 2.5 \text{ MeV}. \qquad (19)$$

The full mass of the Ω_{bbb} is then calculated as

$$M_{\Omega_{bbb}} = \left[E_{\Omega_{bbb}} - \frac{3}{8} (E_{\eta_b} + 3E_\Upsilon) \right]_{\text{LQCD}} + E_{\text{Coulomb}}$$
$$+ \frac{3}{2} [M_\Upsilon]_{\text{PDG}} - \frac{3}{8} [E_\Upsilon - E_{\eta_b}]. \qquad (20)$$

Here, the first term is given by (14), and the last term (the bottomonium hyperfine splitting) is taken from the lattice calculation [37]:

$$E_\Upsilon - E_{\eta_b} = \left[\frac{E_\Upsilon - E_{\eta_b}}{1P \text{ tensor}} \right]_{\text{LQCD}} \cdot [1P \text{ tensor}]_{\text{PDG}}$$
$$= 60.3 \pm 5.5_{\text{stat}} \pm 5.0_{\text{syst}} \pm 2.1_{\text{exp}} \text{ MeV}. \qquad (21)$$

In (21), the ratio of the $1S$ hyperfine splitting and the $1P$ tensor splitting is used [37]. The experimental uncertainty in the $1P$ tensor splitting [63] leads to the last error in (21). In Eq. (20), the mass of the Υ is taken from the Particle Data Group to be $M_\Upsilon = 9.4603 \pm 0.0003$ GeV [63]. The final result for the mass of the Ω_{bbb} is then

$$M_{\Omega_{bbb}} = 14.371 \pm 0.004_{\text{stat}} \pm 0.011_{\text{syst}} \pm 0.001_{\text{exp}} \text{ GeV}. \qquad (22)$$

VI. CONCLUSIONS

The value for $M_{\Omega_{bbb}}$ obtained here, Eq. (22), is compared to results from various continuum calculations in Table IV. The results from the literature range from 13.28 ± 0.10 GeV, calculated using sum rules in [19], to 14.834 GeV calculated using a quark model in [17]. The nonperturbative dynamical lattice QCD calculation performed here, with a total uncertainty of only 12 MeV, is a valuable test of the continuum models. If an experimental

TABLE IV.   Comparison of results for the Ω_{bbb} mass.

Reference	$M_{\Omega_{bbb}}$ (GeV)
Ponce [3]	14.248
Hasenfratz *et al.* [4]	14.30
Bjorken [5]	14.76 ± 0.18
Tsuge *et al.* [6]	13.823
Silvestre-Brac [9]	14.348–14.398
Jia [14]	14.37 ± 0.08
Martynenko [15]	14.569
Roberts and Pervin [17]	14.834
Bernotas and Simonis [18]	14.276
Zhang and Huang [19]	13.28 ± 0.10
This work	$14.371 \pm 0.004_{\text{stat}} \pm 0.011_{\text{syst}} \pm 0.001_{\text{exp}}$

result for $M_{\Omega_{bbb}}$ ever becomes available, it will in turn become a stringent test of the lattice calculation.

The value (22) obtained here satisfies the baryon-meson mass inequality $M_{\Omega_{bbb}} \geq \frac{3}{2} M_\Upsilon$ derived in [64–66], like most of the results given in Table IV, with the exception of those from [6,19].

While the lattice calculation of $M_{\Omega_{bbb}}$ can *rule out* many continuum models, the sole agreement for this value from a model-dependent calculation with several parameters is of course not sufficient to show that the assumptions of that model are correct. To establish the usefulness of a model, multiple predictions using only a small number of parameters need to be tested. It is planned to perform lattice calculations also for excited states of the Ω_{bbb}, which will give more insight into the three-quark forces of QCD. Excited states have been studied using a quark model in [9]. Another direction is the lattice calculation of masses of triply-heavy baryons containing charm quarks: ccc, ccb, and cbb. Lattice NRQCD is not well suited for charm quarks due to their lower mass; instead, for example, the Fermilab method [67] can be used for them.

[1] G. S. Bali, Phys. Rep. **343**, 1 (2001).
[2] N. Brambilla *et al.* (Quarkonium Working Group), CERN Yellow Report No. CERN-2005-005, 2005.
[3] W. Ponce, Phys. Rev. D **19**, 2197 (1979).
[4] P. Hasenfratz, R. R. Horgan, J. Kuti, and J. M. Richard, Phys. Lett. **94B**, 401 (1980).
[5] J. D. Bjorken, FERMILAB Report No. FERMILAB-Conf-85/69, 1985.
[6] M. Tsuge, T. Morii, and J. Morishita, Mod. Phys. Lett. A **1**, 131 (1986); **2**, 283(E) (1987).
[7] J. L. Basdevant and S. Boukraa, Z. Phys. C **30**, 103 (1986).
[8] A. Martin and J. M. Richard, Phys. Lett. B **355**, 345 (1995).
[9] B. Silvestre-Brac, Few-Body Syst. **20**, 1 (1996).
[10] J. Schaffner-Bielich and A. P. Vischer, Phys. Rev. D **57**, 4142 (1998).
[11] J. Vijande, H. Garcilazo, A. Valcarce, and F. Fernandez, Phys. Rev. D **70**, 054022 (2004).
[12] S. Migura, D. Merten, B. Metsch, and H. R. Petry, Eur. Phys. J. A **28**, 41 (2006).
[13] A. Faessler, T. Gutsche, M. A. Ivanov, J. G. Korner, V. E. Lyubovitskij, D. Nicmorus, and K. Pumsa-ard, Phys. Rev. D **73**, 094013 (2006).
[14] Y. Jia, J. High Energy Phys. 10 (2006) 073.
[15] A. P. Martynenko, Phys. Lett. B **663**, 317 (2008).
[16] S. M. Gerasyuta and E. E. Matskevich, Int. J. Mod. Phys. E **17**, 585 (2008).
[17] W. Roberts and M. Pervin, Int. J. Mod. Phys. A **23**, 2817 (2008).
[18] A. Bernotas and V. Simonis, Lithuanian Physics Journal **49**, 19 (2009).
[19] J. R. Zhang and M. Q. Huang, Phys. Lett. B **674**, 28 (2009).
[20] T. T. Takahashi, H. Matsufuru, Y. Nemoto, and H. Suganuma, Phys. Rev. Lett. **86**, 18 (2001).
[21] N. Brambilla, J. Ghiglieri, and A. Vairo, Phys. Rev. D **81**, 054031 (2010).
[22] V. A. Saleev, Mod. Phys. Lett. A **14**, 2615 (1999).
[23] S. P. Baranov and V. L. Slad, Yad. Fiz. **67**, 829 (2004) [Phys. At. Nucl. **67**, 808 (2004)].
[24] M. A. Gomshi Nobary and R. Sepahvand, Phys. Rev. D **71**, 034024 (2005).
[25] M. A. Gomshi Nobary and R. Sepahvand, Nucl. Phys. **B741**, 34 (2006).
[26] R. Lewis and R. M. Woloshyn, Phys. Rev. D **79**, 014502 (2009).
[27] T. Burch, C. Hagen, C. B. Lang, M. Limmer, and A. Schafer, Phys. Rev. D **79**, 014504 (2009).
[28] H. Na and S. Gottlieb, Proc. Sci., LATTICE2008 (2008) 119.
[29] W. Detmold, C. J. Lin, and M. Wingate, Nucl. Phys. **B818**, 17 (2009).
[30] H. W. Lin, S. D. Cohen, N. Mathur, and K. Orginos, Phys. Rev. D **80**, 054027 (2009).
[31] L. Liu, H. W. Lin, K. Orginos, and A. Walker-Loud, Phys. Rev. D **81**, 094505 (2010).
[32] T. W. Chiu and T. H. Hsieh, Nucl. Phys. **A755**, 471 (2005).
[33] S. J. Dong and K. F. Liu, Proc. Sci., LAT2007 (2007) 093.
[34] S. Meinel, W. Detmold, C. J. Lin, and M. Wingate, Proc. Sci., LAT2009 (2009) 105.
[35] B. A. Thacker and G. P. Lepage, Phys. Rev. D **43**, 196 (1991).
[36] G. P. Lepage, L. Magnea, C. Nakhleh, U. Magnea, and K. Hornbostel, Phys. Rev. D **46**, 4052 (1992).
[37] S. Meinel, Phys. Rev. D **82**, 114502 (2010).
[38] C. Allton *et al.* (RBC and UKQCD Collaborations), Phys. Rev. D **76**, 014504 (2007).
[39] C. Allton *et al.* (RBC and UKQCD Collaborations), Phys. Rev. D **78**, 114509 (2008).
[40] A. Bazavov *et al.*, Rev. Mod. Phys. **82**, 1349 (2010).
[41] E. Eichten and B. R. Hill, Phys. Lett. B **240**, 193 (1990).
[42] G. P. Lepage and P. B. Mackenzie, Phys. Rev. D **48**, 2250 (1993).

[43] N. H. Shakespeare and H. D. Trottier, Phys. Rev. D **58,** 034502 (1998).

[44] S. N. Syritsyn *et al.*, Proc. Sci., LATTICE2008 (2008) 169.

[45] A. Bazavov *et al.* (MILC Collaboration), Proc. Sci., LAT2009 (2009) 079.

[46] A. Bazavov *et al.* (MILC Collaboration), Proc. Sci., LAT2009 (2009) 077.

[47] D. B. Kaplan, Phys. Lett. B **288,** 342 (1992).

[48] Y. Shamir, Nucl. Phys. **B406,** 90 (1993).

[49] V. Furman and Y. Shamir, Nucl. Phys. **B439,** 54 (1995).

[50] Y. Iwasaki, Report No. UTHEP-118, 1983.

[51] Y. Iwasaki and T. Yoshie, Phys. Lett. B **143B,** 449 (1984).

[52] Y. Aoki *et al.*, Phys. Rev. D **69,** 074504 (2004).

[53] K. Orginos and D. Toussaint (MILC Collaboration), Phys. Rev. D **59,** 014501 (1998).

[54] G. P. Lepage, Phys. Rev. D **59,** 074502 (1999).

[55] K. Orginos, D. Toussaint, and R. L. Sugar (MILC Collaboration), Phys. Rev. D **60,** 054503 (1999).

[56] M. Lüscher and P. Weisz, Commun. Math. Phys. **97,** 59 (1985); **98,** 433(E) (1985).

[57] M. Lüscher and P. Weisz, Phys. Lett. **158B,** 250 (1985).

[58] M. G. Alford, W. Dimm, G. P. Lepage, G. Hockney, and P. B. Mackenzie, Phys. Lett. B **361,** 87 (1995).

[59] K. C. Bowler *et al.* (UKQCD Collaboration), Phys. Rev. D **54,** 3619 (1996).

[60] G. P. Lepage, B. Clark, C. T. H. Davies, K. Hornbostel, P. B. Mackenzie, C. Morningstar, and H. Trottier, Nucl. Phys. B, Proc. Suppl. **106,** 12 (2002).

[61] S. Meinel, Phys. Rev. D **79,** 094501 (2009).

[62] J. L. Domenech-Garret and M. A. Sanchis-Lozano, Comput. Phys. Commun. **180,** 768 (2009).

[63] C. Amsler *et al.* (Particle Data Group), Phys. Lett. B **667,** 1 (2008).

[64] J. P. Ader, J. M. Richard, and P. Taxil, Phys. Rev. D **25,** 2370 (1982).

[65] S. Nussinov, Phys. Rev. Lett. **51,** 2081 (1983).

[66] J. M. Richard, Phys. Lett. **139B,** 408 (1984).

[67] A. X. El-Khadra, A. S. Kronfeld, and P. B. Mackenzie, Phys. Rev. D **55,** 3933 (1997).